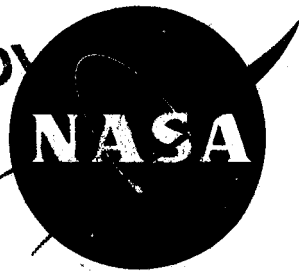


EXTRA COPY



LIBRARY COPY

JAN 5 1961

SPACE FLIGHT  
LANGLEY FIELD, VIRGINIA

# TECHNICAL NOTE

D-634

EFFECTS OF CONE ANGLE, MACH NUMBER, AND NOSE BLUNTING  
ON TRANSITION AT SUPERSONIC SPEEDS

By K. R. Czarnecki and Mary W. Jackson

Langley Research Center  
Langley Field, Va.

NATIONAL AERONAUTICS AND SPACE ADMINISTRATION  
WASHINGTON

January 1961

✓

NATIONAL AERONAUTICS AND SPACE ADMINISTRATION

TECHNICAL NOTE D-634

EFFECTS OF CONE ANGLE, MACH NUMBER, AND NOSE BLUNTING  
ON TRANSITION AT SUPERSONIC SPEEDS

By K. R. Czarnecki and Mary W. Jackson

SUMMARY

An investigation has been made to determine the transition characteristics of a group of blunt cones which varied in included apex angle from  $27^\circ$  to  $60^\circ$  over a Mach number range from 1.61 to 2.20 and a range of tunnel Reynolds number per foot from about  $1.5 \times 10^6$  to  $8.0 \times 10^6$ . The tests were made at zero angle of attack and with zero heat transfer.

The results indicate that the general level of transition Reynolds number based on boundary-layer momentum thickness and local flow conditions just outside the boundary layer varied between 600 and 1,100. Changes in Mach number had little effect on transition distance and transition Reynolds number for the near-sharp or very small bluntnesses. The effect of Mach number variation on the larger hemispherical bluntnesses was much stronger, with the strongest Mach number effect occurring for Mach numbers between 1.61 and 1.82. With an increase in nose radius, there was a strong decrease in transition distance and transition Reynolds number at the lower Mach numbers. This adverse effect tended to become weaker with increase in Mach number. An increase in cone angle at a constant Mach number caused a reduction in transition distance and transition Reynolds number for the blunt configurations which had approximately the same values of nose radius.

INTRODUCTION

The importance of the study of boundary-layer transition has been quite evident in the search for suitably designed configurations of supersonic and hypersonic airplanes and missiles. The state of the art is still such that recourse generally must be had to experimental data in making estimates of transition Reynolds numbers. Although a large body of experimental data is now available for study, there is still a lack of data wherein some of the parameters are varied in a systematic manner and the results are obtained in a single facility in which the apparent turbulence level and local flow irregularities are small.

An investigation has been underway in the Langley 4- by 4-foot supersonic pressure tunnel to supply some of the needed data. This investigation was conducted in two parts. The results of the first part, reported in reference 1, showed the effects of nose angle and Mach number on transition on sharp-nosed cones at supersonic speeds. Further tests have been made to study the transition characteristics of a group of smooth, blunt-nosed cones. The results of this part of the investigation are presented in this report and are compared with those results previously reported in reference 1.

Three basic cones were used in the investigation, with included apex angles of  $27^\circ$ ,  $45^\circ$ , and  $60^\circ$ . Ten blunt-nosed tips, varying from hemispherical to parabolic and hyperbolic shapes, were tested. The test free-stream Mach numbers were 1.61, 1.82, 2.01, and 2.20. The tunnel Reynolds number per foot varied from about  $1.5 \times 10^6$  to  $8.0 \times 10^6$ . All data were taken with the models at zero angle of attack and with zero heat transfer. Transition was determined by means of schlieren photography.

#### SYMBOLS

$M_\infty$	free-stream Mach number
$M_\lambda$	local Mach number at outer edge of boundary layer
$r$	nose radius
$s_{tr}$	surface distance to transition measured from stagnation point
$s_f$	fictitious surface distance to transition for blunt-nosed cones measured from apex of sharp-nosed cone
$\theta$	boundary-layer momentum thickness
$R_\lambda$	Reynolds number based on local conditions at outer edge of boundary layer
$R_\theta$	Reynolds number based on momentum thickness and local conditions at outer edge of boundary layer
$R_{\theta, tr}$	transition Reynolds number based on momentum thickness and local conditions at outer edge of boundary layer

## APPARATUS AND METHODS

### Wind Tunnel

This investigation was conducted in the Langley 4- by 4-foot supersonic pressure tunnel, which is a rectangular, closed-throat, single-return tunnel with provisions for the control of pressure, temperature, and humidity of the enclosed air. Flexible nozzle walls were adjusted to give the desired test-section Mach numbers of 1.61, 1.82, 2.01, and 2.20. During the tests, the dewpoint was kept below  $-20^{\circ}$  F at atmospheric pressure; therefore, the effects of water condensation in the supersonic nozzle were negligible.

### Models

The basic models used in this investigation (fig. 1) were two 24.00-inch-long sharp-nosed cones whose apex angles measured  $27^{\circ}$  and  $45^{\circ}$ , and one 17.50-inch-long sharp-nosed cone whose apex angle measured  $60^{\circ}$ . The base of the  $60^{\circ}$  cone was modified by cutting down and beveling in order to obtain an effective decrease in area ratio so that the tunnel would start at least at the highest test Mach number. A photograph of these models is presented as figure 2. In order to facilitate changes in nose shapes, each basic model was made in two parts. Care was taken that the joints between the parts were faired smooth to lessen the effects of surface irregularities. Additional information concerning the basic models is given in reference 1.

Detailed sketches of the blunt-tip configurations for this investigation are presented in figure 3. These configurations consist of three general family shapes: the hemispherical, the hyperbolic, and the parabolic. Nose tips for the cone configurations with  $27^{\circ}$  apex angle consisted of three hemispherical nose shapes whose radii measured 0.247 inch, 0.710 inch, and 1.234 inches; one parabolic nose shape; and one hyperbolic nose shape. One hemispherical nose shape, with a 1.345-inch radius, was tested for the model with  $45^{\circ}$  apex angle. The model with  $60^{\circ}$  apex angle had one parabolic nose shape and three hemispherical nose shapes whose radii measured 0.50 inch, 1.25 inches, and 2.00 inches.

All models were constructed of solid steel and were polished to a mirrorlike finish which, from past experience represents a surface roughness of less than 5 microinches root mean square. All models were sting mounted for the tests.

## Tests

All tests were conducted with the models at zero angle of attack. The  $27^\circ$  configurations were tested at free-stream Mach numbers of 1.61, 1.82, 2.01, and 2.20. The  $45^\circ$  configurations were tested at free-stream Mach numbers of 2.01 and 2.20 and the  $60^\circ$  configurations were tested at a free-stream Mach number of 2.20 only, because of tunnel choking. Tunnel stagnation pressures varied from about 800 to 4,300 pounds per square foot which correspond to tunnel Reynolds numbers per foot ranging from about  $1.5 \times 10^6$  to  $8.0 \times 10^6$ . The tunnel stagnation temperatures varied from about  $95^\circ$  F to  $130^\circ$  F.

Test procedure consisted of starting at low tunnel stagnation pressures and advancing to the higher pressures. Whenever data were to be recorded, the tunnel was brought to and held at the desired tunnel conditions and then schlieren photographs were made. Light flashes of approximately 4 microseconds were used to obtain the photographs. Figure 4 presents typical schlieren photographs showing the location of transition. Since equilibrium conditions existed at the time the data were recorded, there was no transfer of heat.

## Data Reduction

The location of transition was determined by visual inspection of the schlieren photographs by two or more readers. The transition locations determined by the different readers were then averaged at each tunnel stagnation pressure and the average value was then treated as a single test point. In most instances the differences in the transition locations determined by the various readers were negligible. Boundary-layer momentum thickness for the sharp-nosed configurations, for which the data were presented in reference 1 and with which the blunted configurations of the present investigation are compared, was computed by the Chapman and Rubesin technique (ref. 2). Mangler's transformation (ref. 3), which gives the general relationship between two-dimensional and axially symmetrical boundary layers, was used to reduce the flat-plate calculations to those for a conical body. Flow conditions on the conical surfaces were obtained with the aid of the tables in reference 4, with the assumption that no boundary layer was present. The pressure distribution over the nose of the blunted configurations has been calculated according to modified Newtonian theory which gives good agreement with experimental data for hemispherical bodies at Mach number of 2.0 or higher. Cone theory was employed to secure the pressures on the conical sections of the models. Boundary-layer characteristics for the blunted configurations were calculated by the basic approach of reference 5, which presents a technique for calculating the compressible laminar boundary layer that is applicable to flows with arbitrary pressure gradient.

## RESULTS AND DISCUSSION

The discussion of data obtained during this investigation is divided into two general sections: transition distance and transition Reynolds number. The four parameters varied in this investigation are as follows: Reynolds number per foot, Mach number, nose bluntness, and cone apex angle. The results of the tests are presented in the form of plots of transition distance or transition Reynolds number as a function of the fundamental parameter, local Reynolds number per foot. The other parameters are discussed with reference to these plots. Because the transition results for the sharp-nosed cones of reference 1 are intimately connected with and form a convenient reference base for the discussion of the results of the present blunt-nosed tests, they are treated as an integral part of the present investigation.

### Transition Distance

Effect of Mach number.- The effect of Mach number on surface distance to transition  $s_{tr}$  for the blunt-nosed cones is shown in figure 5. Only the  $27^\circ$  configurations (fig. 5(a)) were investigated at all the test Mach numbers of 1.61, 1.82, 2.01, and 2.20 because of the tunnel choking problem with the larger cones at the lower Mach numbers. In addition, the  $45^\circ$  cone with its limited configurations was tested at Mach numbers of 2.01 and 2.20 (fig. 5(b)). Included in each plot are two lines: a short-dash line indicating the surface length of the respective configuration, and a long-dash  $45^\circ$  or diagonal line representing the average transition distances for the sharp-nosed configurations and indicating the slope corresponding to a constant transition Reynolds number. The diagonal line for the sharp-nosed configuration has been repeated at the same position on all plots as a reference for comparison of decrease or increase of surface transition distance with respect to the effect of Mach number for the other configurations. A symbol with an arrow indicates that in some instances transition occurred off the base of the model and the true average is somewhat higher than the value plotted. For some test conditions, transition appeared to oscillate back and forth on the model and concentrated at two different locations. Two symbols, indicating the averaged forward and aft locations of transition, joined by a vertical line indicate this occurrence. It should be noted that for the Reynolds number range investigated, transition occurred on the conical section of the models and in no instance reached the blunted portion of the models.

The slope of the transition distance data for the configurations investigated was approximately parallel (within experimental accuracy generally) to the curve of the reference constant transition Reynolds

number except for Reynolds numbers per foot above approximately  $6 \times 10^6$ . Above this Reynolds number, at Mach number 1.61, the data show a consistent abrupt decrease in the distance to transition. This phenomenon may be attributed to the adverse pressure gradient existing just behind the juncture of the blunt nose and the cone. At the higher Mach numbers, the results appear to indicate a similar abrupt decrease in the distance to transition above  $R_L$  per foot =  $6 \times 10^6$  for some of the configurations investigated (notably, the hemispherical-nosed models with  $r = 0.247$  inch and  $r = 1.234$  inches and the hyperbolic-nosed model at Mach number 1.82; and the hemispherical-nosed model with  $r = 1.345$  inches at Mach number 2.20). Inspection of the results for smaller or larger nose bluntnesses and smaller or larger Mach numbers shows that this trend is not consistent. Also, this high Reynolds number per foot range where the transition-distance decrease appears to occur is a region where the actual transition location is difficult to locate accurately on the schlieren photographs. This difficulty is a consequence of the thin boundary layers involved near the tip of the model and the large amount of graininess appearing over the photographs because of the turbulent boundary layer on the tunnel windows. The lack of effect of Reynolds number per foot on transition, which appears contrary to experiences in other wind tunnels (for example, see ref. 6), is in line with results of other recent tests in this tunnel (ref. 1) and with results of reference 7.

The effect of Mach number on the transition distance  $s_{tr}$  for the  $27^\circ$  cone configurations was small for the sharp-nosed cones, but it increased rapidly in magnitude as the nose bluntnesses of the hemispherical configurations were increased. For example, as the nose radius was increased from the sharp-nose value of about 0.001 inch or 0.002 inch to a radius of 0.247 inch, the effect of changes in Mach number became discernible in the lowest Mach number range. As the nose radius was increased further to 0.710 inch, the effect of Mach number became stronger and the Mach number influence was extended upward to Mach number 2.01. For the case of the largest hemispherical bluntness tested, the Mach number effects were even stronger, but the data indicate that the strongest region of influence was still in the lowest Mach number range. For this most blunt configuration (hemispherical-nosed model with  $r = 1.234$  inches), an increase in Mach number from 1.61 to 2.01 or 2.20 resulted in an increase in transition distance of more than 100 percent.

The effect of Mach number on the hyperbolic-nosed and parabolic-nosed configurations was about as might be expected for their bluntnesses relative to the bluntnesses of the hemispherical-nosed cones. For the hyperbolic configuration, which in general appearance lies somewhere between the sharp and the 0.247-inch-radius hemispherical-nosed configuration (fig. 3), there was little if any Mach number effect

except for the abrupt decrease in transition distance above a Reynolds number per foot of  $6 \times 10^6$  at the lower Mach numbers. In relative bluntness, the parabolic configuration appears to lie between the 0.247-inch-radius and the 0.710-inch-radius hemispherical noses (fig. 3); and the effect of Mach number on transition, which may be noted only at Mach number 1.61, appears to fall roughly within the range of effects on these two configurations for Reynolds numbers per foot which are below that for the abrupt transition-distance decrease.

An examination of the results for the  $45^\circ$  cone (fig. 5(b)), indicates that Mach number had little effect on transition distance for the sharp-nosed cone and a somewhat larger effect on transition distance for the blunter cone. This is the same trend as was noted for the  $27^\circ$  configurations.

The apparent decrease in transition distance at the lower values of Reynolds number per foot is not understood, but previously such a decrease has been found to occur near the base of sharp-nosed models (ref. 1).

Effect of nose blunting.- The effect of nose blunting on surface distance to transition for all blunted configurations tested is shown in figure 6. The figure is divided into three parts: (a) the  $27^\circ$  configurations, (b) the  $45^\circ$  configurations, and (c) the  $60^\circ$  configurations. The reference lines for constant transition Reynolds number and model length are also included in this figure.

The data for the blunt  $27^\circ$  configurations clearly indicate the abrupt decrease in transition distance in the range above Reynolds numbers per foot of  $6 \times 10^6$  and emphasize the concentration of the decrease at Mach number 1.61. Below this region of abrupt decrease in transition distance, the data also indicate that nose blunting has its largest effect on decreasing transition distance at the lowest Mach number. Blunting the sharp nose to a 1.234-inch radius decreased the transition distance approximately 60 percent at Mach number 1.61. At Mach number 2.20, the decrease in transition distance for the same change in bluntness was only 20 to 30 percent of the transition distance for the sharp-nosed model. The parabolic nose bluntness caused a slight decrease in transition distance at Mach number 1.61 and there was little if any effect above that Mach number. This result might be expected from the general shape of the parabolic nose. Changing from the sharp to the more blunt but still relatively sharp hyperbolic configuration did not show any effect of blunting on transition distance within the test Mach number range.



Data for the  $45^\circ$  configurations (fig. 6(b)) and the  $60^\circ$  configurations (fig. 6(c)), for the most part, follow trends similar to those of the previously discussed  $27^\circ$  cones (fig. 6(a)).

The results shown herein concerning a decrease in transition distance with an increase in nose bluntness are substantiated by the results of reference 8, so long as transition distance is less than 100 tip radii downstream from the tip.

Effect of cone angle.- Figure 7 is presented so that an analysis may be made of the effect of cone angle on transition distance for configurations with approximately the same values of nose radius at a constant Mach number. Although the nose radii of the different hemispherical configurations investigated are not identical, their measurements (approximately 1.3 inches) are considered close enough to be comparable and the effects of differences in their measurements are assumed to be negligible. This comparison of data is made primarily at Mach number 2.20; however, additional data at Mach number 2.01 are included. The data at Mach number 2.20 show that an increase in cone angle results in a decrease in transition distance for configurations of approximately the same values of nose radius. This observation is supported by the results at Mach number 2.01. Still further corroboration of this trend is found by noting that for the parabolic nose shape at Mach number 2.20, increasing the cone angle from  $27^\circ$  (fig. 6(a)) to  $60^\circ$  (fig. 6(c)) led to a decrease in transition distance.

Another feature of interest indicated by the data of figure 6 is that the effect of increasing cone angle was greater at Mach number 2.01 than at Mach number 2.20. This suggests that the greatest effect of cone angle on transition distance would occur in the Mach number range even lower than 2.01 where the effects of Mach number and nose blunting were also maximum.

Correlation of results.- The results of an attempt to correlate the transition-distance data on the basis of local Mach number just outside the boundary layer are presented in figure 8. These data were obtained by fitting a straight line which had the same slope as the line for constant transition Reynolds number to the test points of figures 5 to 7 and picking off the transition distance indicated by this line at a Reynolds number per foot of  $4 \times 10^6$ . Abrupt decreases in transition distance, such as occurred at free-stream Mach number 1.61 at the high test Reynolds number, and gradual decreases (relative to the line for constant transition Reynolds number) such as occurred for several of the models as transition neared the model base were ignored. As a result, in some cases, there may be a question as to how representative the transition distances thus derived may actually be. In addition to the present results, some data are included from an

unpublished investigation made at the same facility on a sharp-nosed cone with apex angle of  $10^\circ$  at free-stream Mach numbers of 1.41 and 2.01.

The data indicate that, in general, there is some tendency for the transition results to correlate on the basis of local Mach number if the cones have equal bluntness. This is exemplified by the tendency of the sharp-nosed-cone data and the  $r \approx 1.25$ -inch-cone data to fall relatively close to one another. Thus, the effect of cone angle can be explained to some extent by the change in local conditions with changes in cone angle. Changes in local Mach number are not the primary explanation, however, for the effects of bluntness.

### Transition Reynolds Number

Effect of Mach number.- The effect of Mach number on transition Reynolds number  $R_{\theta, tr}$ , based on momentum thickness and local conditions outside the boundary layer, for the six  $27^\circ$  cone configurations is presented in figure 9(a). As in figure 5, the two  $45^\circ$  cone configurations are also included (fig. 9(b)) for purposes of comparison. The effect of Mach number on transition Reynolds number approximates the trend of the effect of Mach number on transition distance. Data for the configurations with sharp, hyperbolic, and 0.247-inch-radius hemispherical noses show an insignificant effect of Mach number on transition Reynolds number for Reynolds numbers per foot which are below that for the abrupt decrease in transition distance. There is, however, a noticeable increase in the effect of Mach number for the larger bluntnesses, and as discussed in the section entitled "Transition Distance," the strongest Mach number effect is concentrated in the range between Mach number 1.61 and Mach number 1.82. Above Reynolds numbers per foot of about  $6 \times 10^6$ , data for the blunted configurations show a dropoff in  $R_{\theta, tr}$  at Mach number 1.61. For the most blunt  $27^\circ$  configuration ( $r = 1.234$  inches), an increase in Mach number from 1.61 to 2.01 or 2.20 caused an increase in  $R_{\theta, tr}$  from about 650 to about 980 or about 50 percent. Data for the  $27^\circ$  parabolic configuration also exhibit an increase in  $R_{\theta, tr}$ . The  $45^\circ$  configurations (fig. 9(b)) further corroborate the trend.

Effect of nose blunting.- Figure 10 shows the effect of nose blunting on transition Reynolds number. The data for the  $27^\circ$  configurations indicate that with an increase in nose bluntness there is a decrease in transition Reynolds number which is strongest at the lowest Mach number, and which tends to become weaker with increase in Mach number. (Note changes in levels of  $R_{\theta, tr}$  curves with changes in  $M_\infty$  for the various nose bluntnesses.) Small bluntnesses, up to the 0.710-inch-radius configuration, exhibited a small but consistent increase in

$R_{\theta, tr}$  over that obtained for the sharp-nosed configuration at constant Mach number for the test Mach numbers above 1.61. At Mach number 1.61 the blunter  $27^\circ$  configurations (0.710-inch-radius and 1.234-inch-radius hemispherical noses) show a relatively smaller  $R_{\theta, tr}$  than the sharp-nosed configuration. Data for the  $45^\circ$  configurations and the  $60^\circ$  configurations further corroborate the trend indicated by the data for the  $27^\circ$  configuration as to the effect of nose blunting. In general, except for the bluntest nose cones where the Mach number effect was strongest, the transition data for all configurations fell in a range of  $R_{\theta, tr}$  from about 800 to 1,100. Thus it appears that, to a first order, the results for the sharper noses appear to correlate fairly well on the basis of a Reynolds number formed from the boundary-layer momentum thickness and the local conditions just outside the boundary layer on the conical section of the models. In reference 8 it is implied that the effect of nose blunting can be explained to a first order on a basis of a constant transition Reynolds number  $R_{\theta, tr}$ . The results from this investigation indicate that this is not true in the lower Mach number range, although it may tend to become more true at higher test Mach numbers.

Effect of cone angle.- The effect of cone angle on transition Reynolds number for configurations with approximately the same values of nose radius at a constant Mach number is shown in figure 11. The data at Mach number 2.20 indicate that an increase in cone angle decreases the transition Reynolds number at a constant Reynolds number per foot. Data for the tests at Mach number 2.01 support this finding. As stated previously in the discussion of the effect of cone angle on transition distance, it appears that the effect of increasing cone angle is greater at Mach number 2.01 than at Mach number 2.20. This fact leads to a general conclusion similar to that of the previous cone-angle discussion that the greatest effect of cone angle on transition Reynolds number would occur in the Mach number range even lower than 2.01 where the effects of Mach number and nose blunting are also maximum. Whereas the transition-distance data did correlate in terms of local Mach number, the data for the different cone configurations with approximately the same value of nose radius did not correlate on the basis of  $R_{\theta, tr}$ , which was computed by a method that took into account local conditions along the surface of the body.

These results for cone angles with a fairly large nose radius are somewhat in contrast to the results of reference 1 which reports there was a relatively small cone-angle effect for the sharp-nosed cones.

Computation of  $R_{\theta}$ .- In trying to correlate the data by using  $R_{\theta}$ , two methods of computing boundary-layer momentum thickness were used.

For the sharp-nosed configurations, the Chapman and Rubesin technique (ref. 2), which does not allow for pressure gradient, was used; for the blunt-nosed configurations, the Cohen and Reshotko technique (ref. 5), which does allow for pressure gradient, was used. One of the basic differences in the two techniques is the assumption made in the Cohen and Reshotko method that the stagnation pressure throughout the flow field behind the detached shock is everywhere the same as that behind the normal shock. Because of the curvature of the detached shock and the consequent generation of a flow field over the model with increasing stagnation pressure with distance from the model surface, it is obvious that this assumption is not correct for points fairly far back on the model where the boundary layer has grown sufficiently to penetrate this outer region. Also, the assumption deteriorates progressively as Mach number is increased.

For the sharp-nosed cones, the shock is straight and the stagnation pressure behind the shock is constant and can be calculated accurately by the use of tables such as those presented in reference 4. Since behind a normal shock the stagnation pressure drops off very rapidly with increase in Mach number, the question arises whether the assumption concerning the use of the stagnation pressure behind the normal shock might result in fairly large differences in boundary-layer characteristics between the blunt-nosed configurations and the sharp-nosed configurations, particularly in the region several diameters back on the model.

Results of the momentum-thickness calculations for the  $27^\circ$  configurations by the two techniques are presented in figure 12. Computations by both techniques at the lowest Mach number where the difference in the assumed and the real stagnation pressure distribution is not great and at the highest Mach number where the difference is larger are presented. A diagonal line having a slope of one-half on the logarithmic plot shows the momentum-thickness curve for the  $27^\circ$  sharp-nosed configuration as a function of surface distance measured from the apex of the  $27^\circ$  sharp nose. Momentum thickness for the three values of nose radius for the hemispherical configurations are plotted as functions of a fictitious surface distance which is the distance to the apex of the extended cone of the conical afterbody. The surface-distance parameter was chosen because all values of  $\theta$  tended to come together in a common straight line for all surface locations on the conical sections of the models. If the values of  $\theta$  for a configuration with a sharp or near-sharp nose were extrapolated from the momentum-thickness curves computed by the Cohen and Reshotko technique, there would be very little difference between the value of  $\theta$  for the sharp-nosed configuration thus obtained and the value of  $\theta$  for the blunted configurations at a given distance on the conical section.

A comparison of the extrapolated values of  $\theta$  for the sharp-nosed configuration with the computed Chapman and Rubesin values shows that at the lowest Mach number there is only a small difference while at the highest Mach number the difference between the two values is quite large. Because this difference is very small at Mach number 1.61, where Mach number and nose bluntness effects are greatest, the effect on correlation of data of using the different techniques is small or even negligible. At Mach number 2.20, where the effects of Mach number and nose blunting on transition distance appeared diminished, the difference in values of  $\theta$  computed by the two techniques may have a significant effect on the correlation. For example, a correction for the difference would improve the correlation of the larger cone angle of figure 11; however, any attempt to make a correction to the data of the  $27^\circ$  cone configuration would be detrimental.

### CONCLUSIONS

An investigation has been made to determine the transition characteristics of a group of blunt-nosed cones which varied from  $27^\circ$  to  $60^\circ$  in included apex angle. Tests were conducted over a Mach number range from 1.61 to 2.20 and a range of tunnel Reynolds number per foot from  $1.5 \times 10^6$  to  $8.0 \times 10^6$ . The results indicate:

1. The general level of transition Reynolds number, based on boundary-layer momentum thickness and local flow conditions just outside the boundary layer, varied between 600 and 1,100.
2. The effects of Mach number, nose bluntness, and cone angle on transition distance and transition Reynolds number were interdependent upon one another.
3. Within the test Mach number range, changes in Mach number had little effect on transition distance and transition Reynolds number for the near-sharp or very small nose bluntnesses, but there was a noticeable increase in effect for the larger hemispherical nose bluntnesses. The strongest Mach number effect was concentrated between Mach number 1.61 and Mach number 1.82.
4. An increase in nose bluntness caused a decrease in transition distance and transition Reynolds number. This effect was strongest at the lowest Mach number and tended to become weaker with increase in Mach number.

5. An increase in cone angle at a constant Mach number caused a reduction in transition distance and transition Reynolds number for the blunt configurations having approximately the same values of nose radius.

Langley Research Center,  
National Aeronautics and Space Administration,  
Langley Field, Va., September 20, 1960.

#### REFERENCES

1. Czarnecki, K. R., and Jackson, Mary W.: Effects of Nose Angle and Mach Number on Transition on Cones at Supersonic Speeds. NACA TN 4388, 1958.
2. Chapman, Dean R., and Rubesin, Morris W.: Temperature and Velocity Profiles in the Compressible Laminar Boundary Layer With Arbitrary Distribution of Surface Temperature. Jour. Aero. Sci., vol. 16, no. 9, Sept. 1949, pp. 547-565.
3. Mangler, W.: Boundary Layers With Symmetrical Airflow About Bodies of Revolution. Rep. No. R-30-18, pt. 20, Goodyear Aircraft Corp., Mar. 6, 1946.
4. Staff of the Computing Section, Center of Analysis (under direction of Zdeněk Kopal): Tables of Supersonic Flow Around Cones. Tech. Rep. No. 1 (Nord Contract No. 9169), M.I.T., 1947.
5. Cohen, Clarence B., and Reshotko, Eli: The Compressible Laminar Boundary Layer With Heat Transfer and Arbitrary Pressure Gradient. NACA Rep. 1294, 1956. (Supersedes NACA TN 3326.)
6. Ross, Albert O.: Determination of Boundary-Layer Transition Reynolds Numbers by Surface-Temperature Measurement of a  $10^\circ$  Cone in Various NACA Supersonic Wind Tunnels. NACA TN 3020, 1953.
7. Van Driest, E. R., and McCauley, W. D.: The Effect of Controlled Three-Dimensional Roughness on Boundary-Layer Transition at Supersonic Speeds. Jour. Aero/Space Sci., vol. 27, no. 4, Apr. 1960, pp. 261-271, 303.
8. Rogers, Ruth H.: The Effect of Tip Bluntness on Boundary-Layer Transition on a  $15^\circ$  Included Angle Cone at  $M = 3.12$  and  $3.81$ . Tech. Note No. Aero 2645, British R.A.E., Aug. 1959.

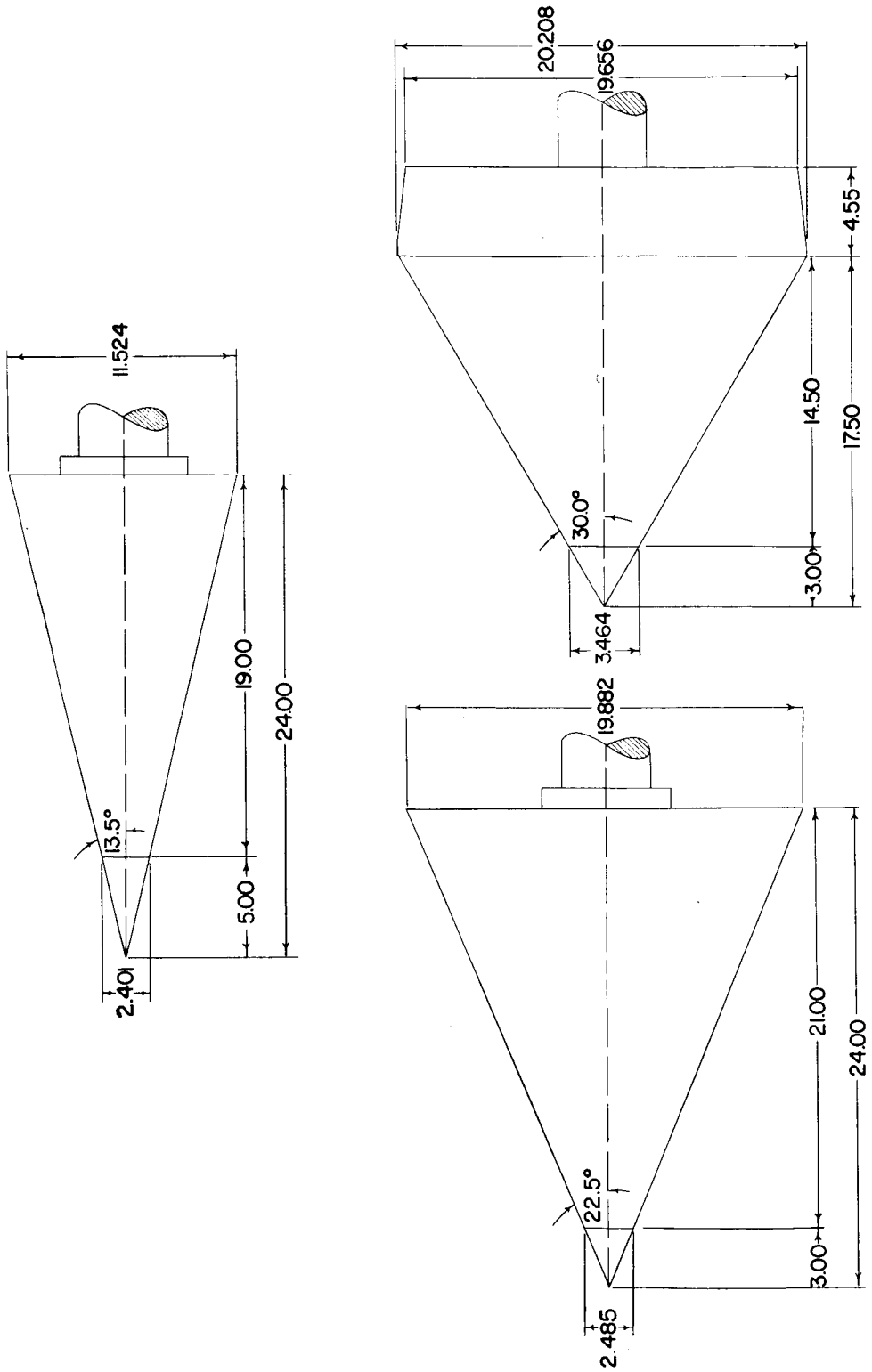


Figure 1.- Basic models. All dimensions are in inches unless otherwise indicated.

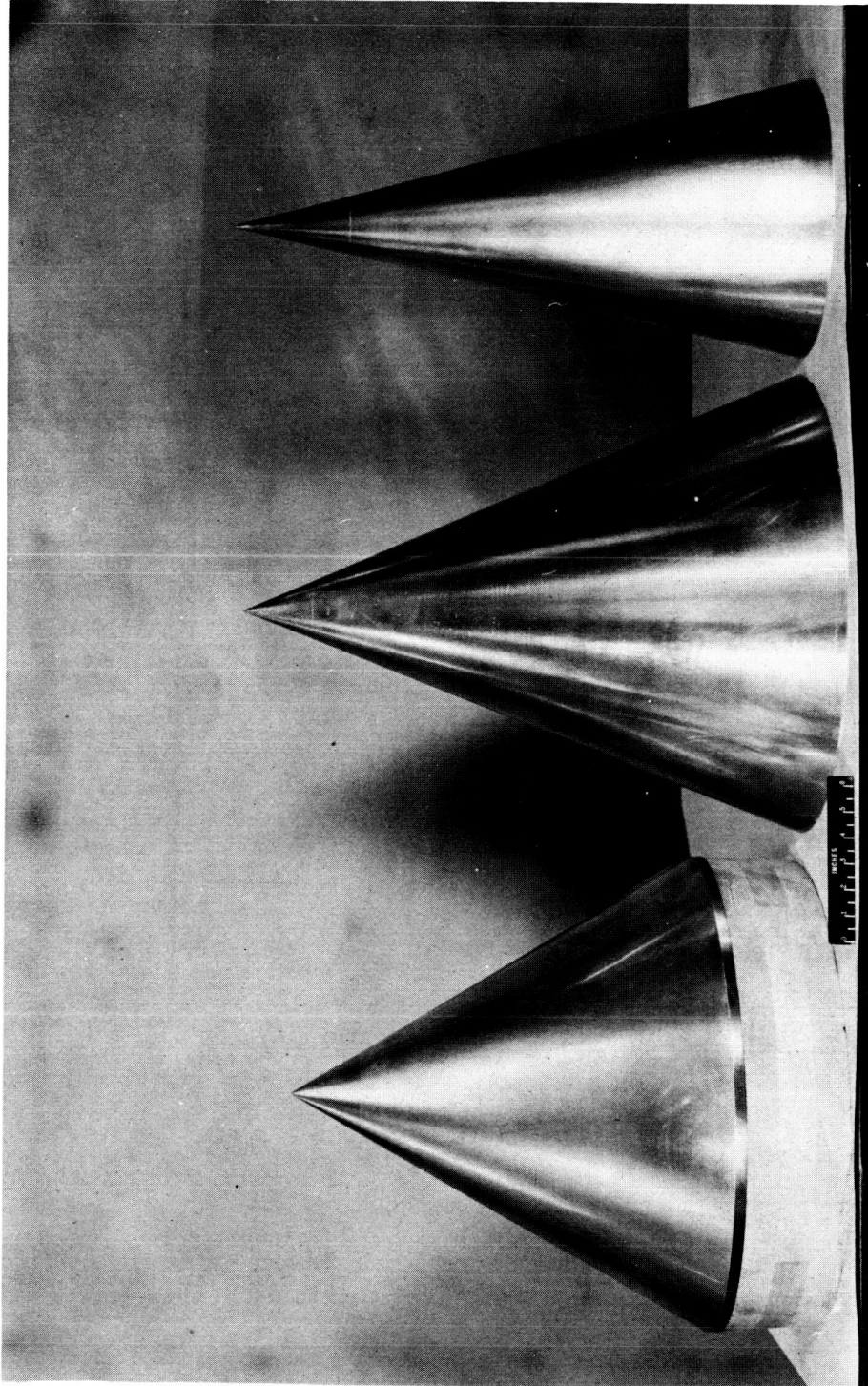
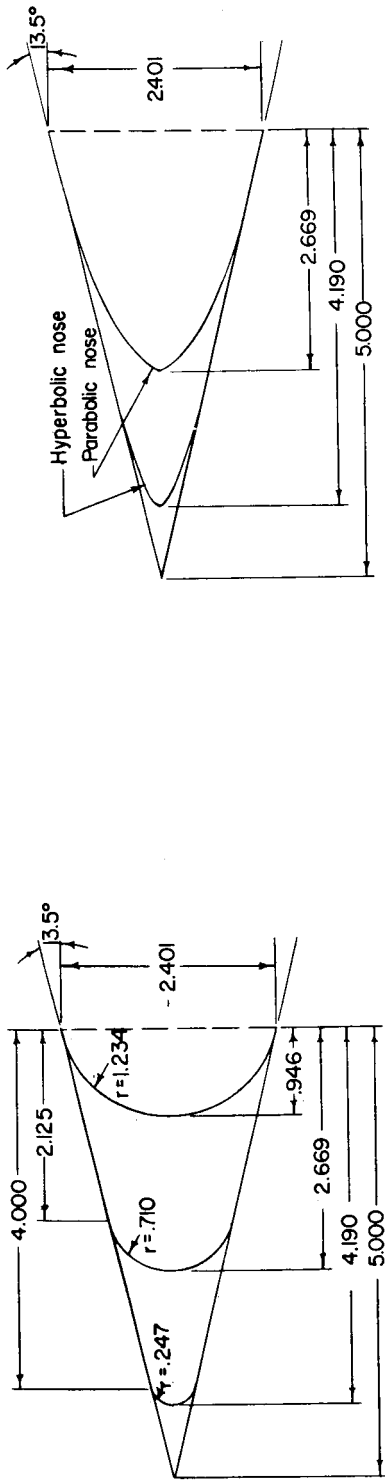


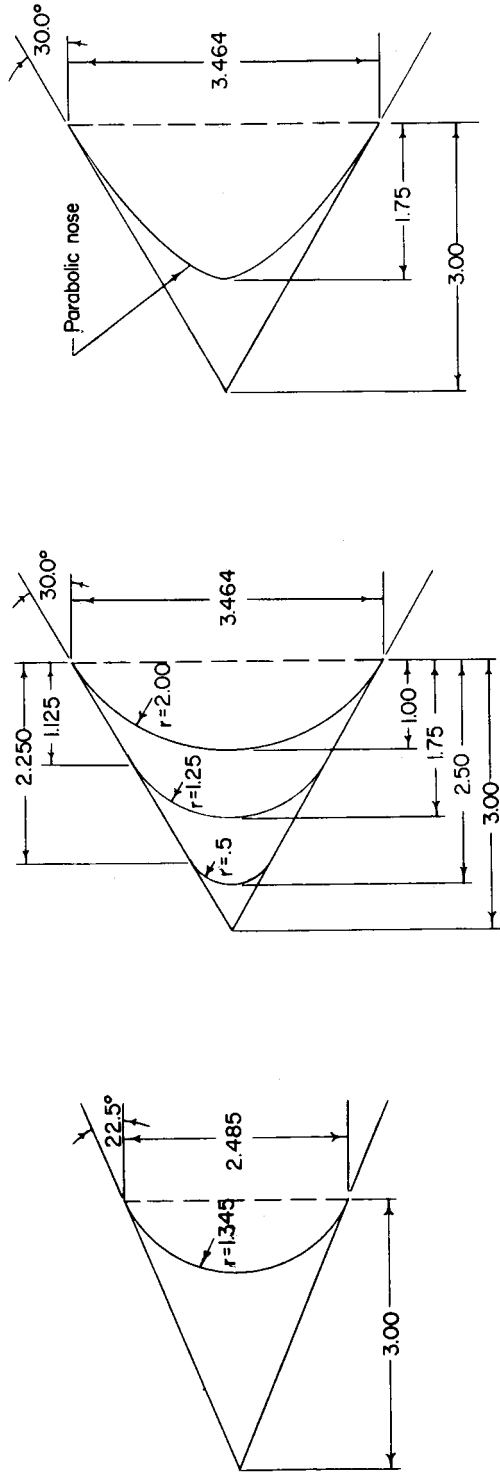
Figure 2.- Photograph of basic models.

L-57-5604

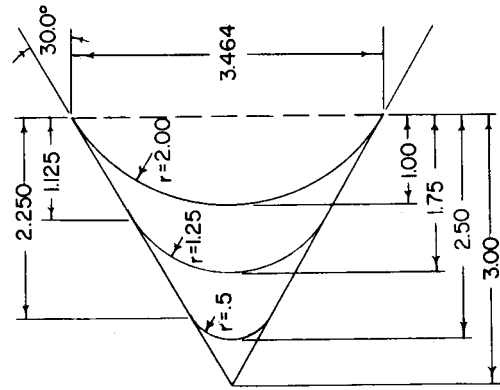




(a) 27° cone configurations.

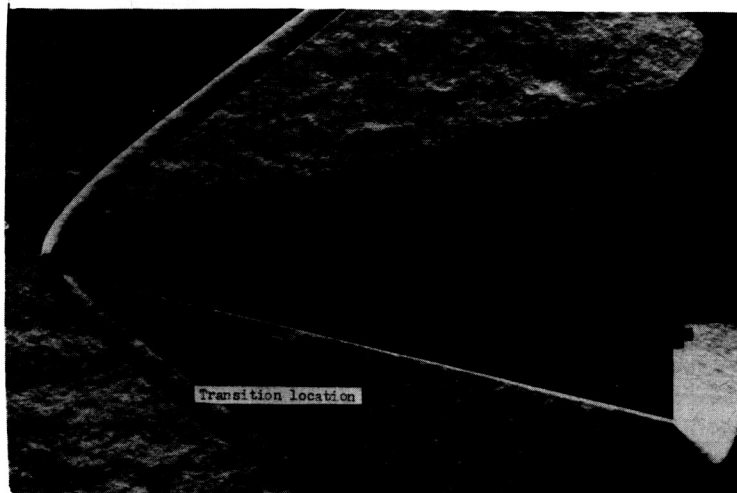


(b) 45° cone configuration.

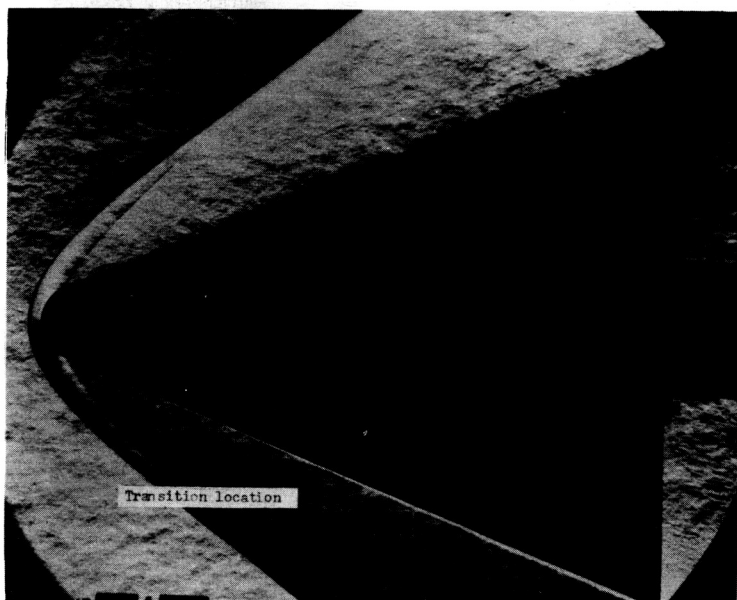


(c) 60° cone configurations.

Figure 3.- Tip configurations used in investigation. All dimensions are in inches unless otherwise indicated.



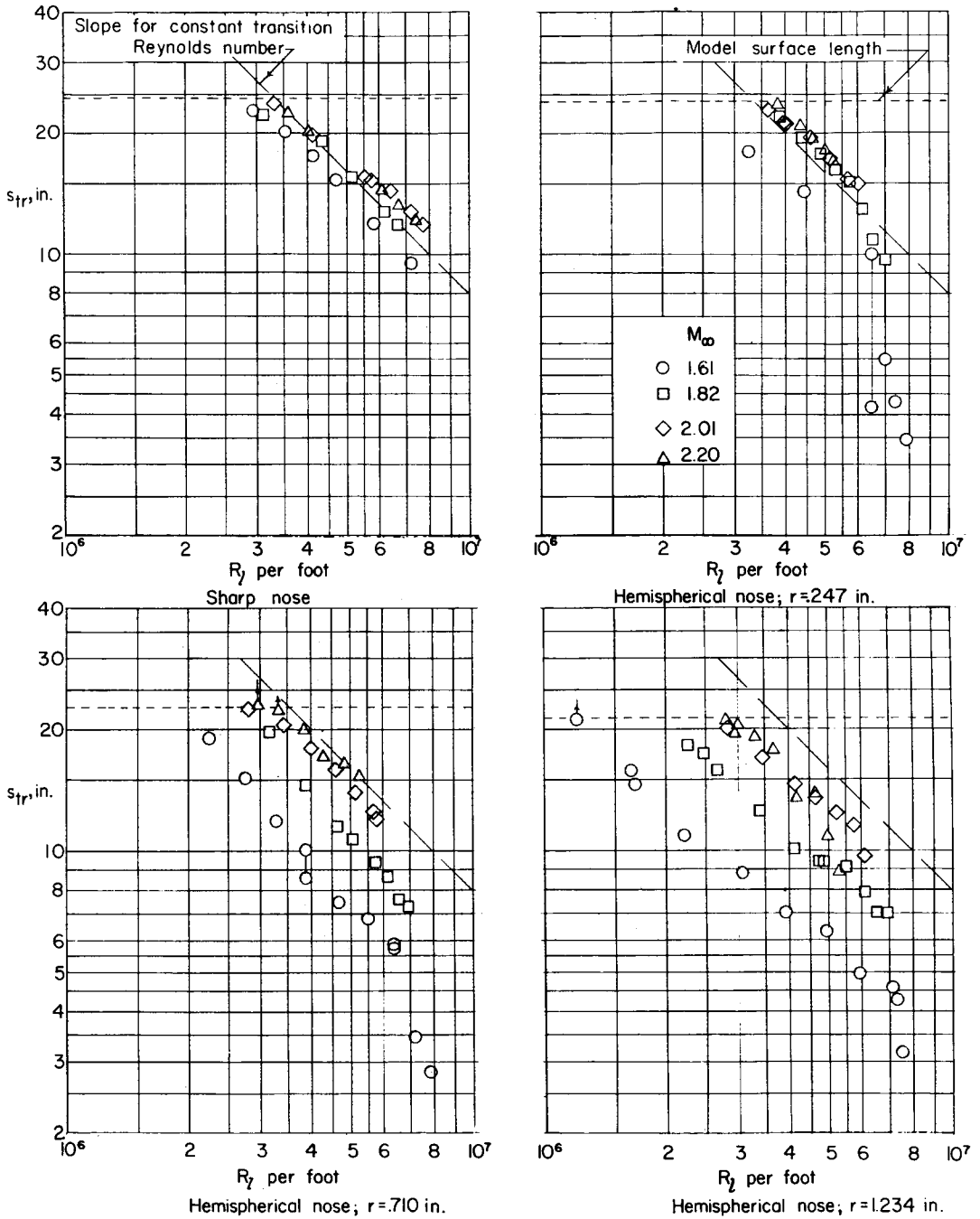
(a) 27° cone configuration.  $r = 0.710$  inch;  $M_\infty = 1.82$ ;  
 $R_\lambda$  per foot =  $5.31 \times 10^6$ .



(b) 45° cone configuration.  $r = 1.345$  inch;  $M_\infty = 2.01$ ;  
 $R_\lambda$  per foot =  $5.29 \times 10^6$ .

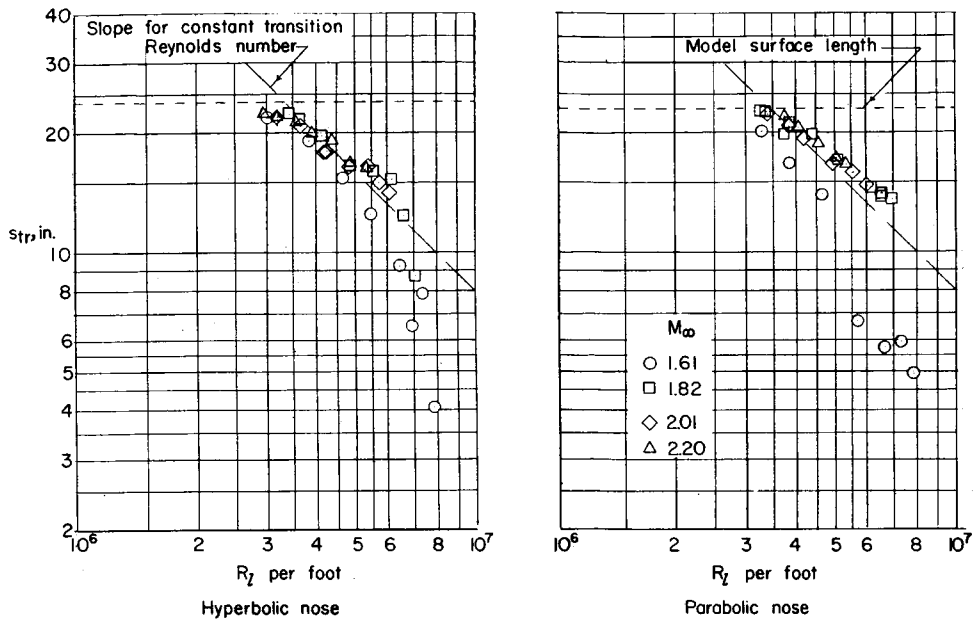
L-60-5581

Figure 4.- Typical schlieren photographs showing location of transition.

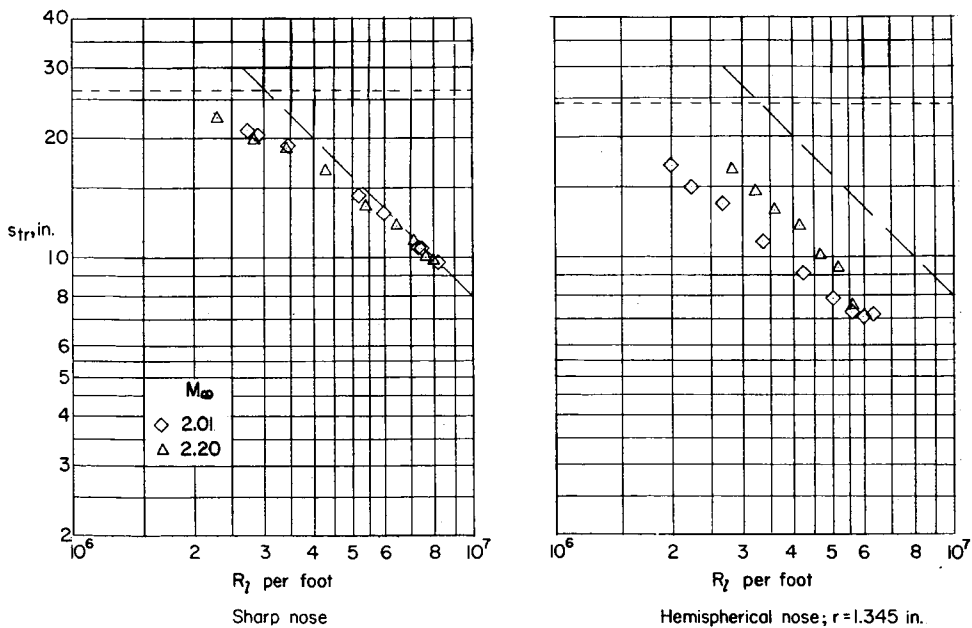


(a)  $27^\circ$  cone configurations.

Figure 5.- Effect of Mach number on surface distance to transition.

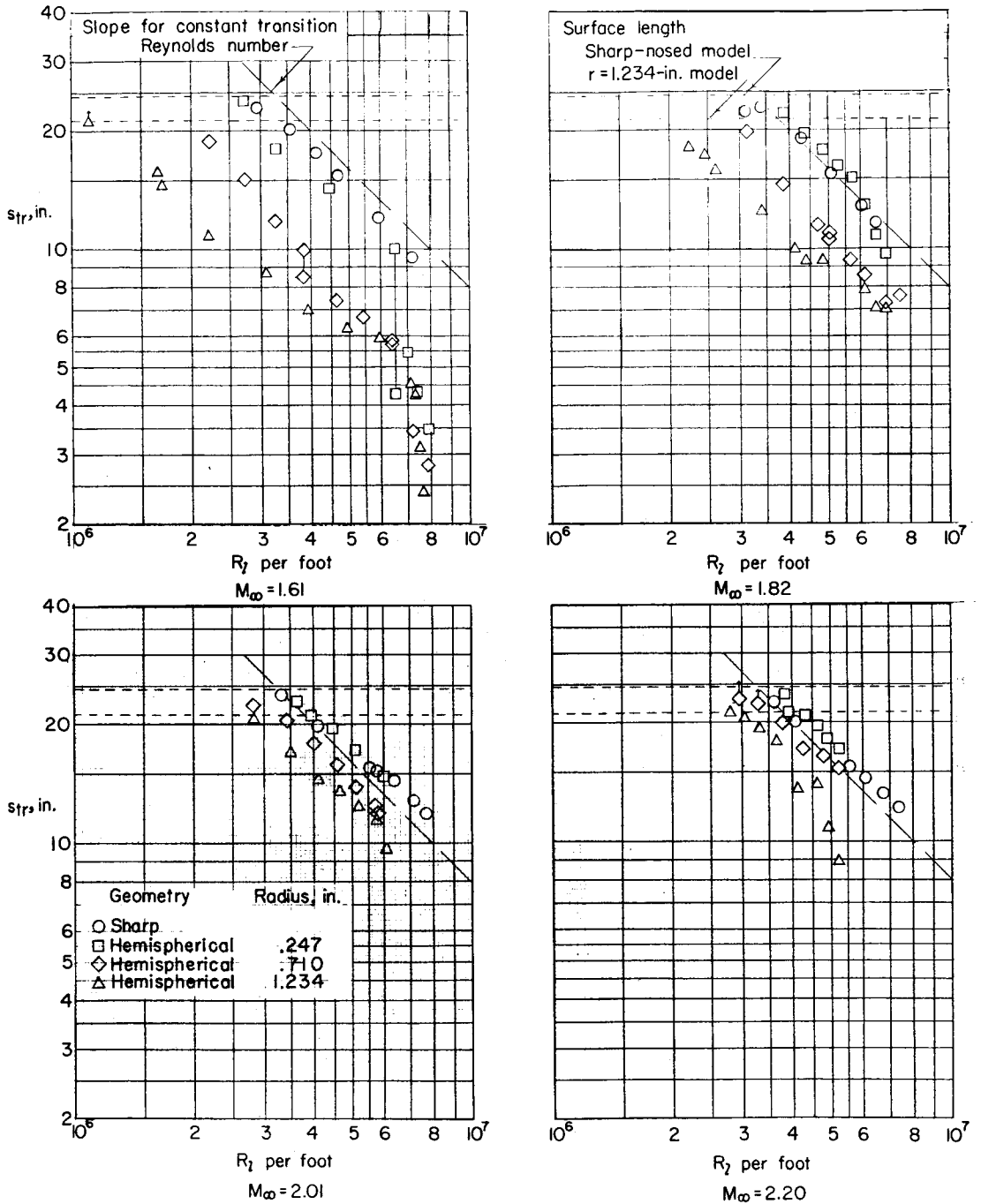


(a)  $27^\circ$  cone configurations. Concluded.



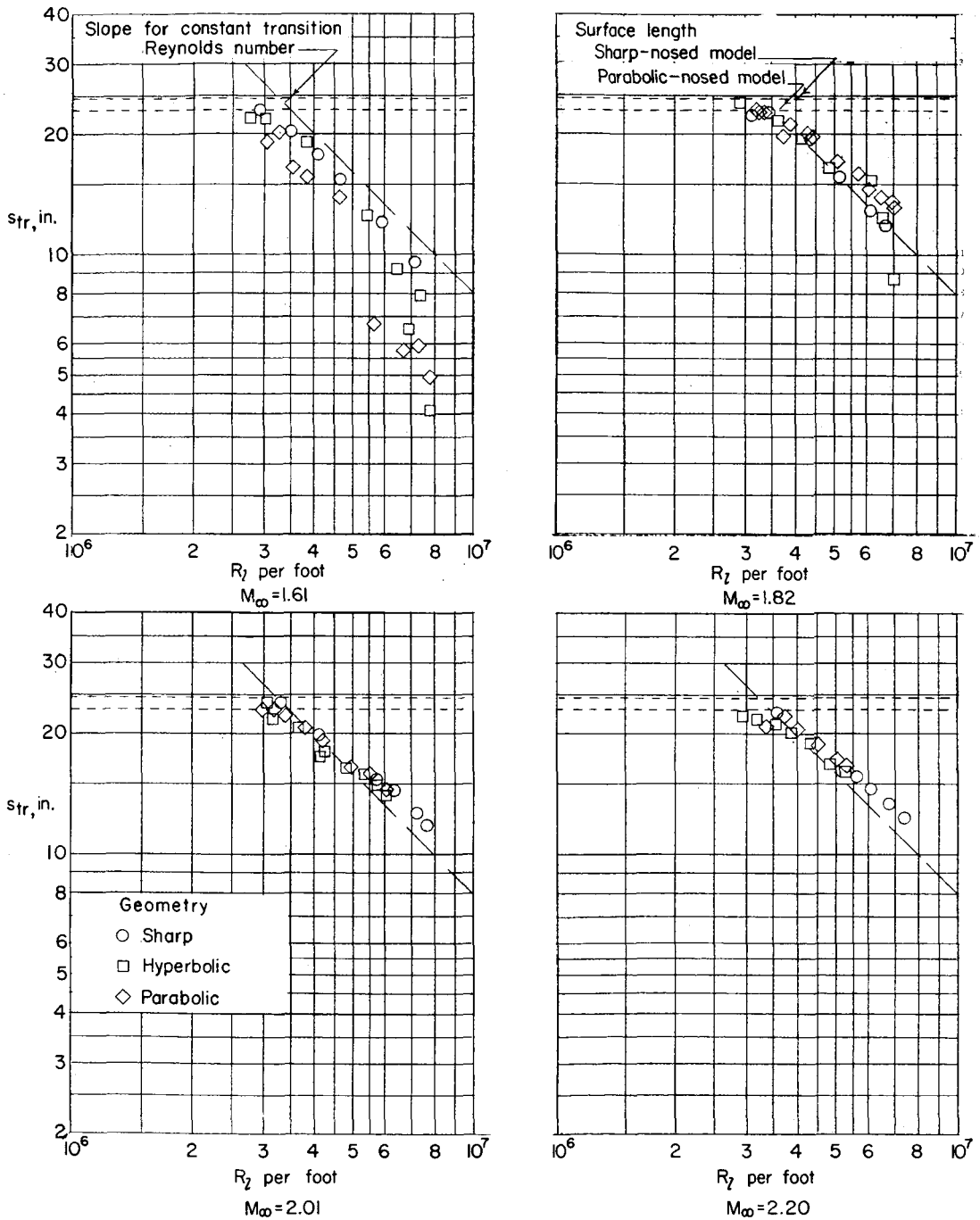
(b)  $45^\circ$  cone configurations.

Figure 5.- Concluded.



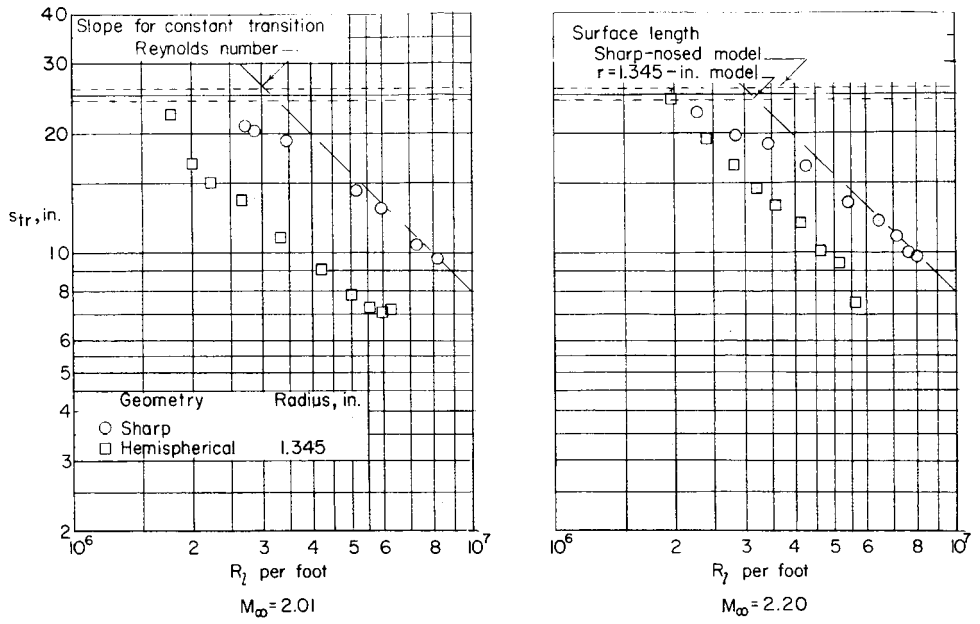
(a)  $27^\circ$  cone configurations.

Figure 6.- Effect of nose blunting on surface distance to transition.

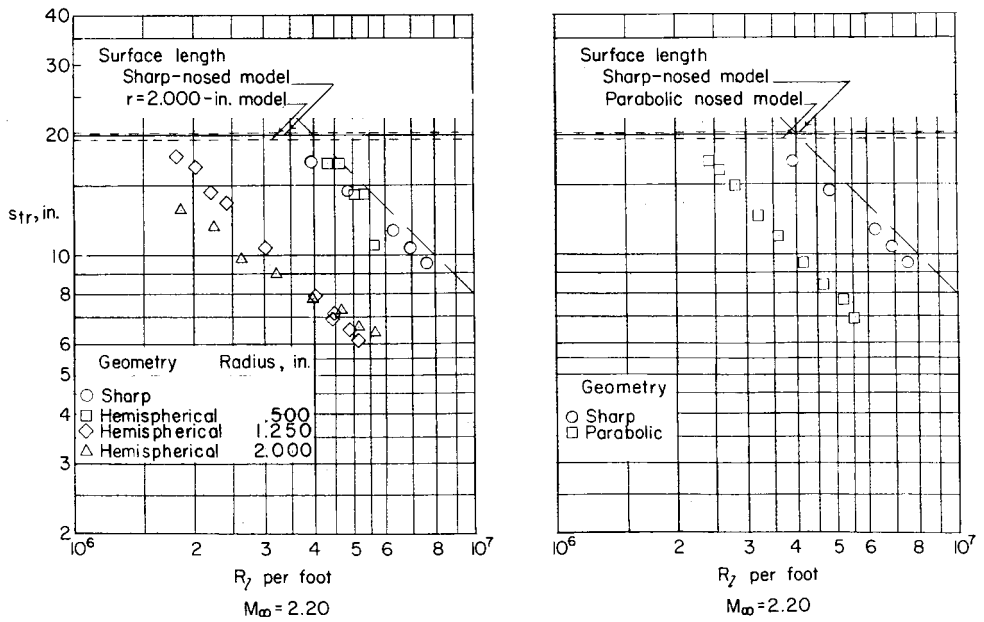


(a)  $27^\circ$  cone configurations. Concluded.

Figure 6.- Continued.



(b)  $45^\circ$  cone configurations.



(c)  $60^\circ$  cone configurations.

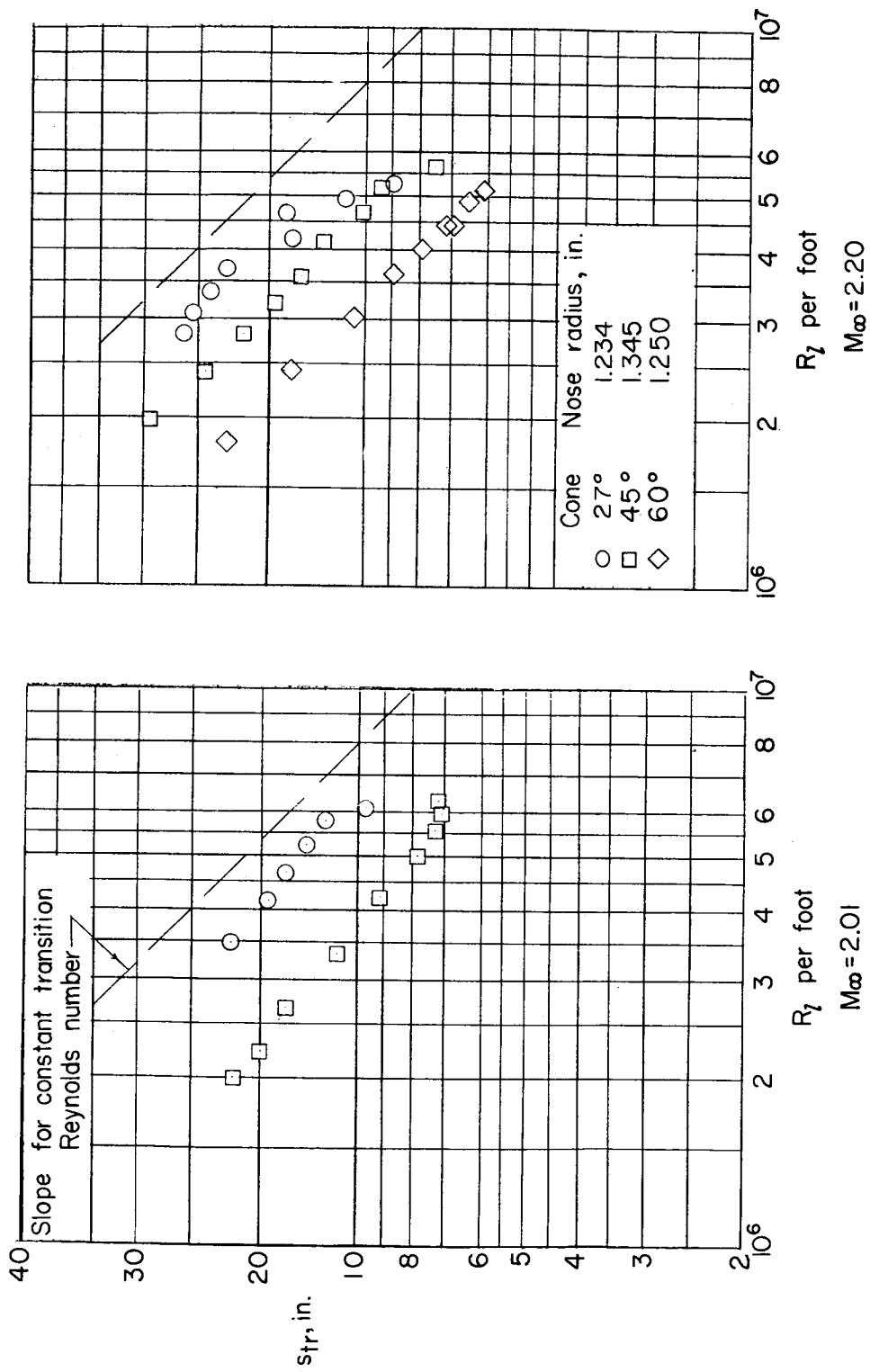


Figure 7.- Effect of cone angle on surface distance to transition for configurations with approximately the same values of nose radius.



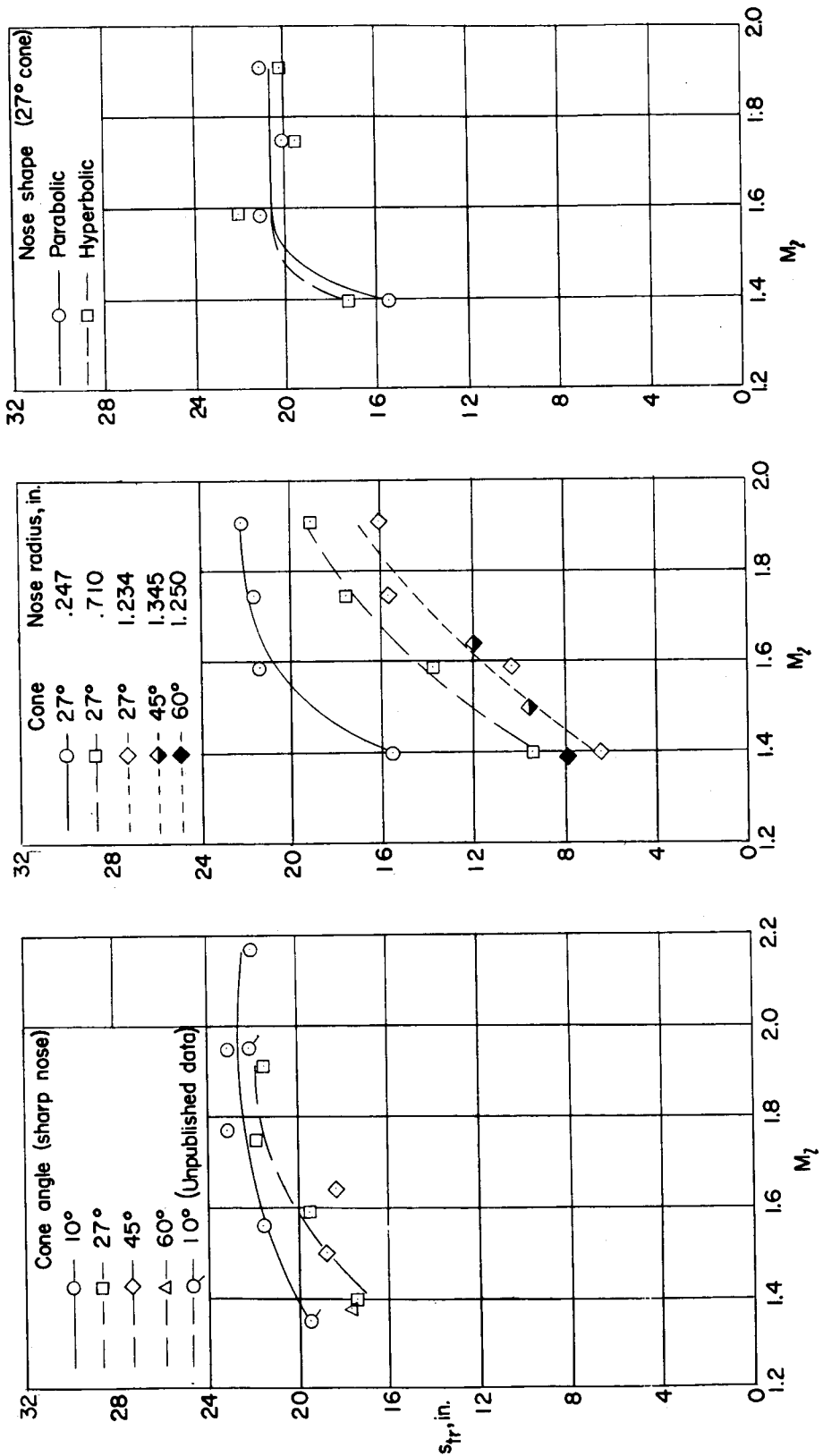


Figure 8.- Correlation of surface distance to transition as a function of local Mach number.  
 $R_1$  per foot =  $4 \times 10^6$ .

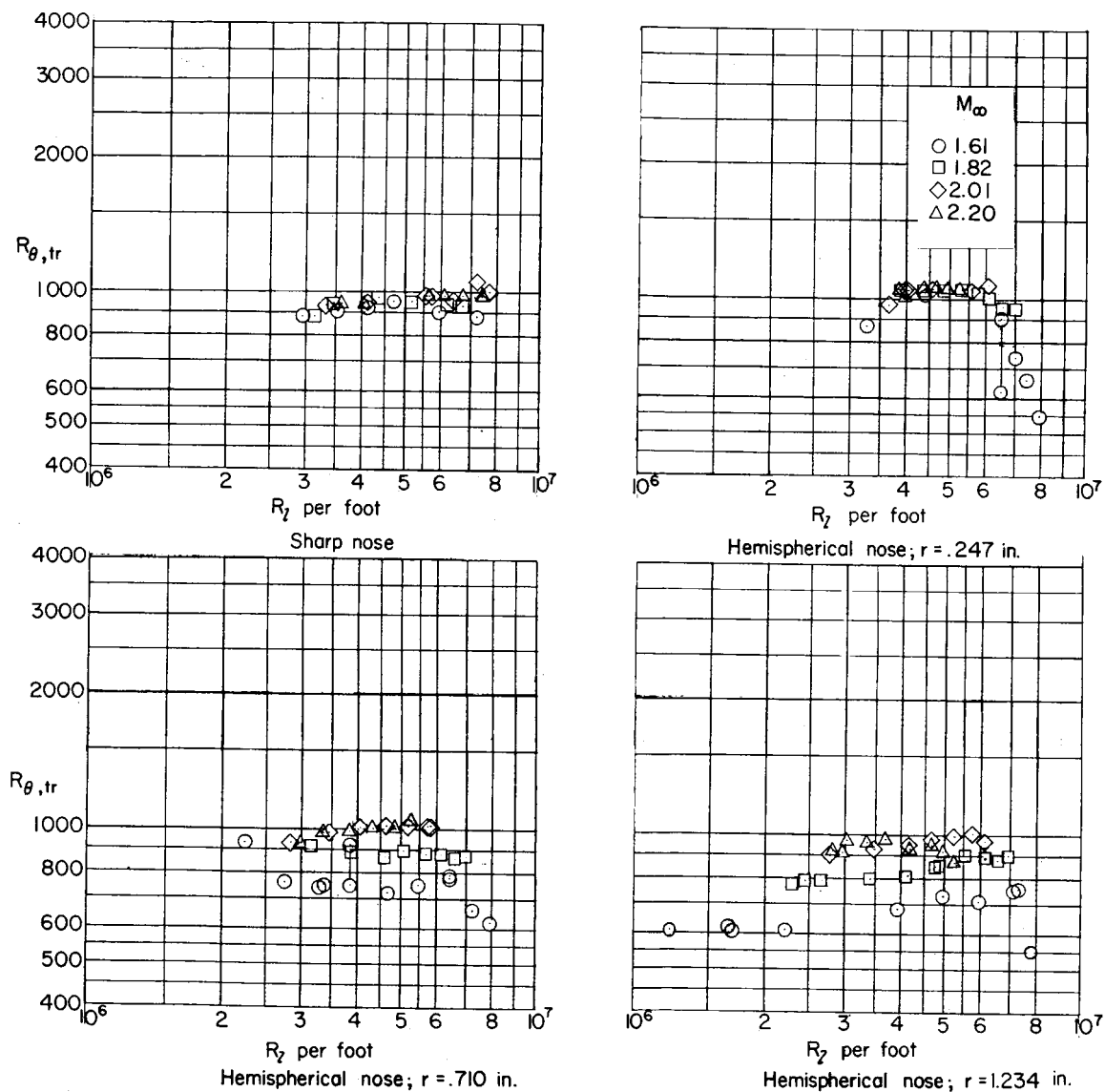
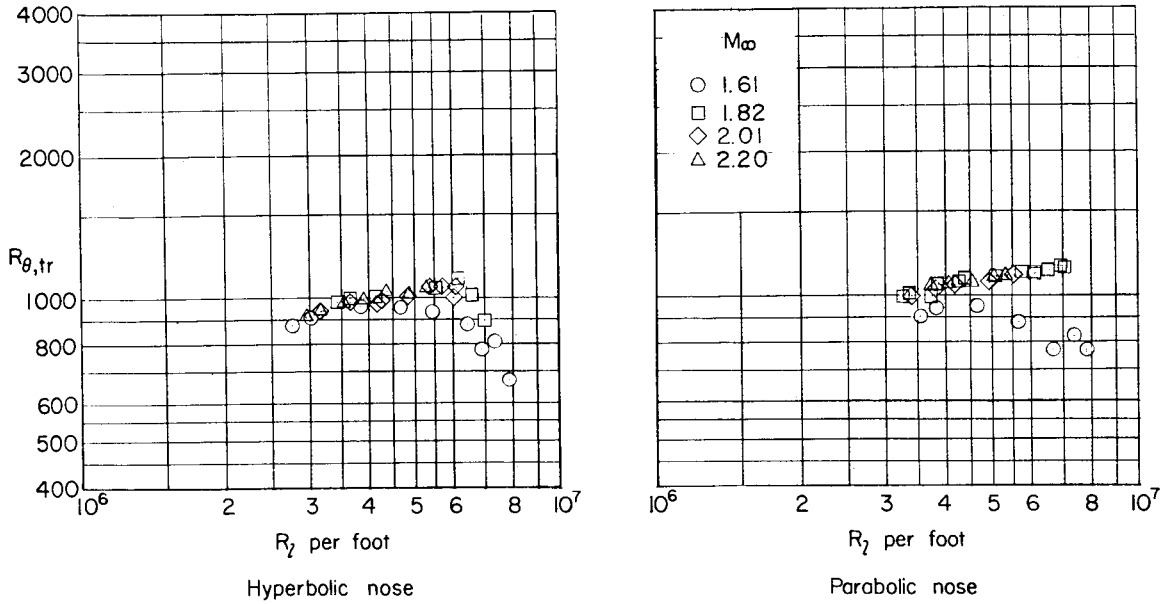
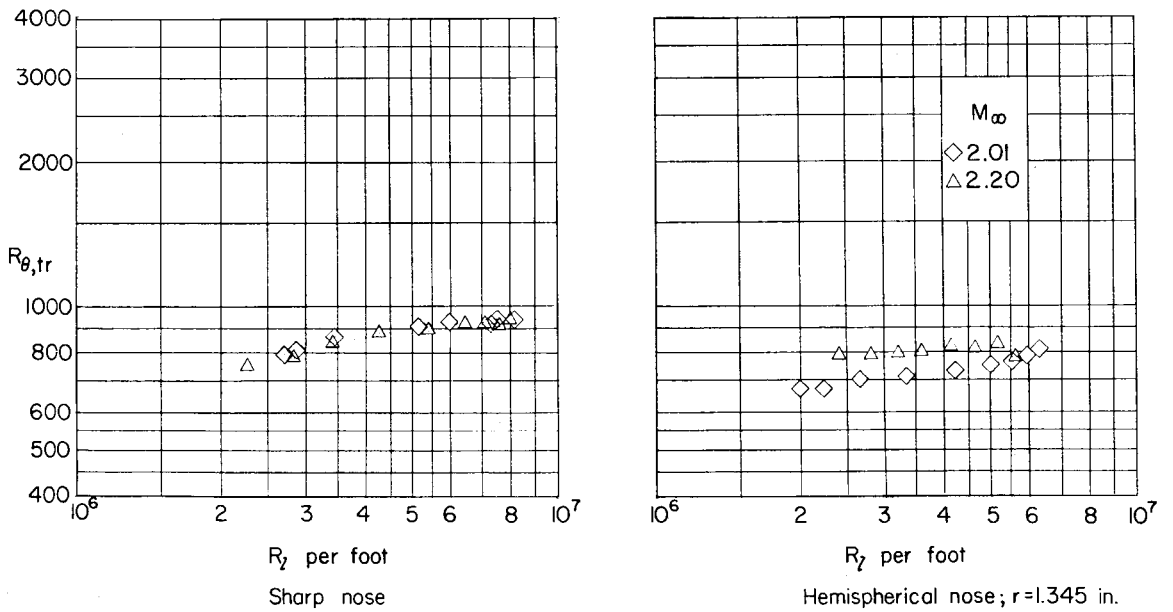
(a)  $27^\circ$  cone configurations.

Figure 9.- Effect of Mach number on transition Reynolds number.

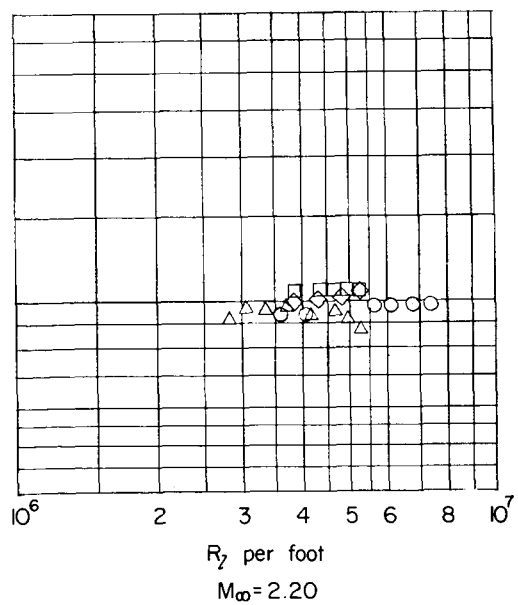
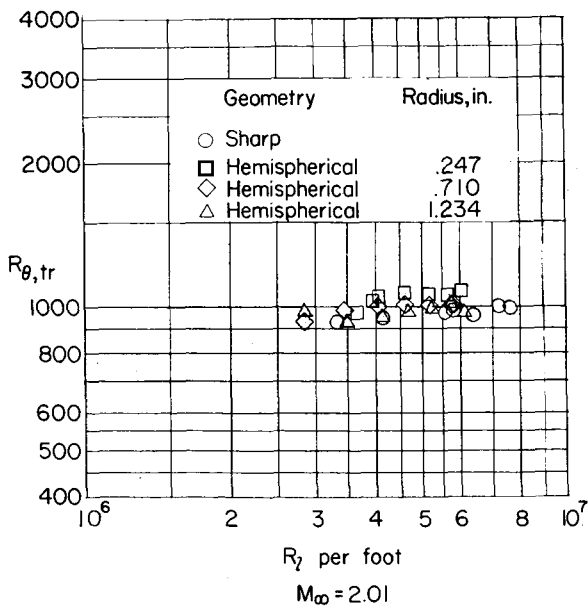
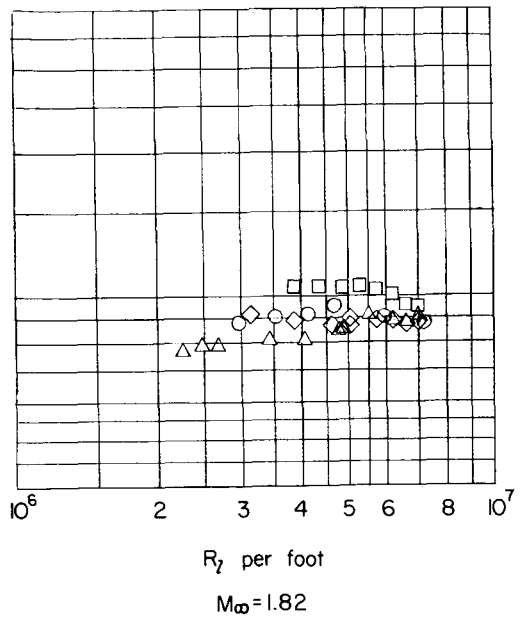
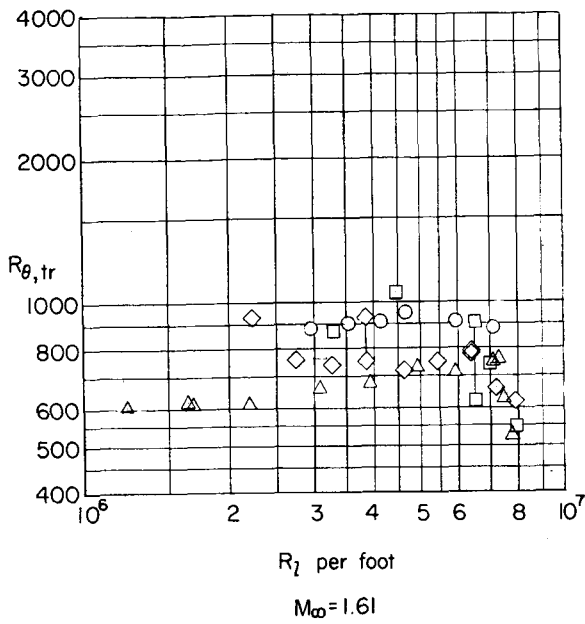


(a)  $27^\circ$  cone configurations. Concluded.



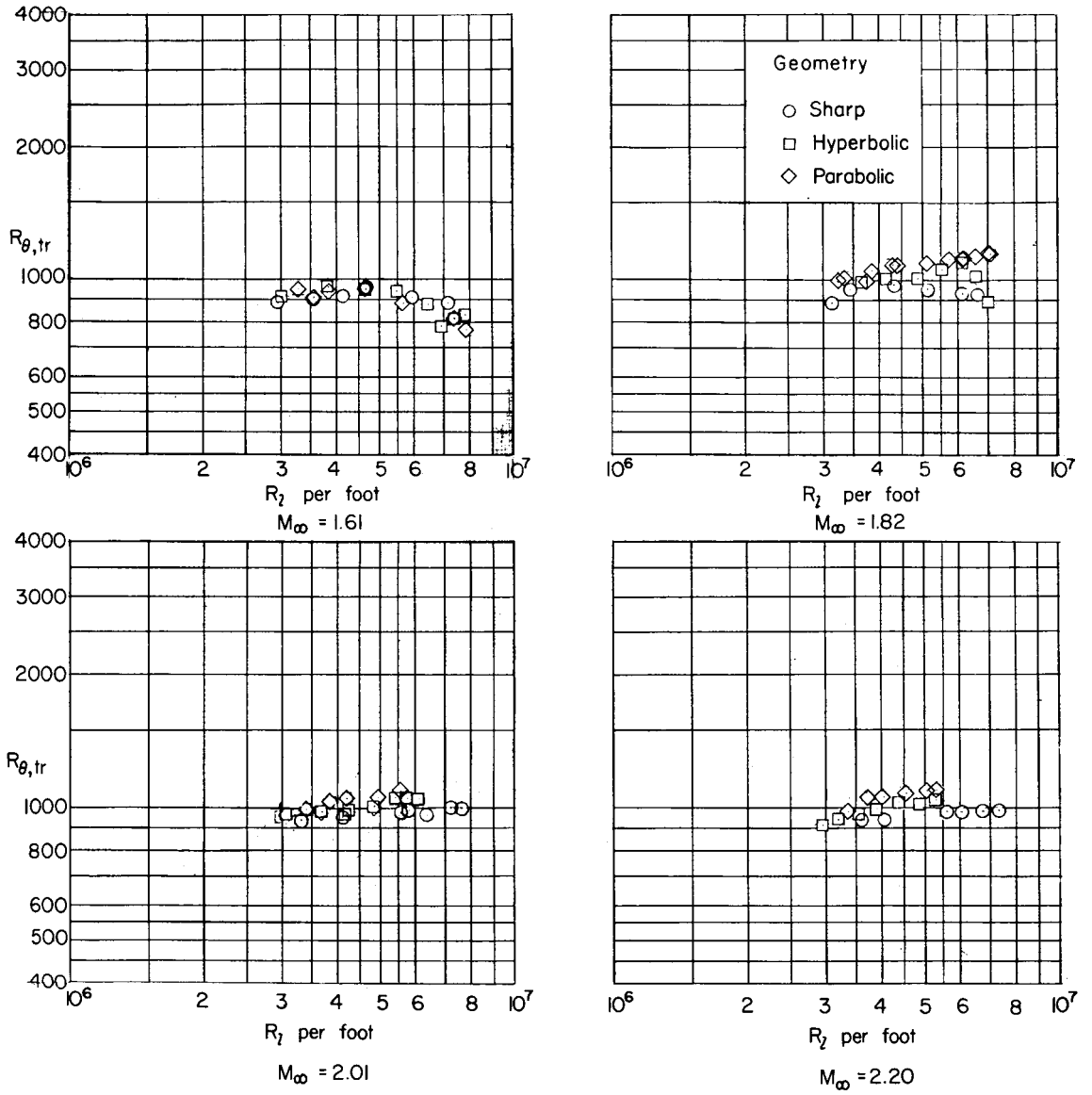
(b)  $45^\circ$  cone configurations.

Figure 9.- Concluded.



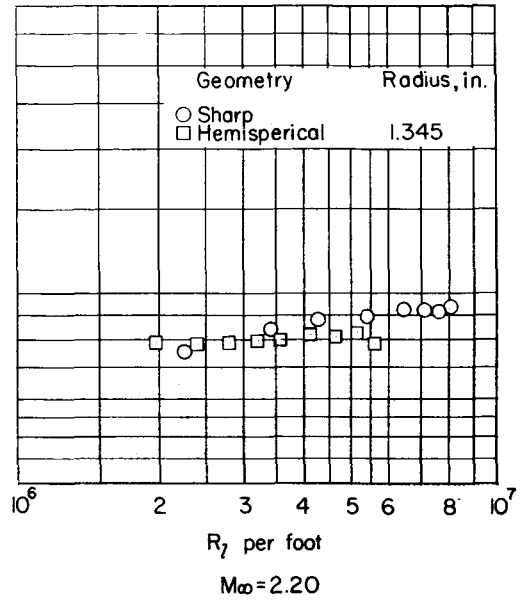
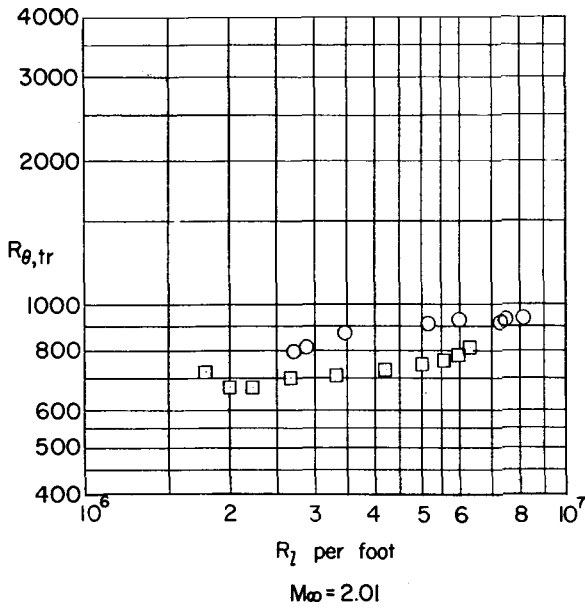
(a)  $27^\circ$  cone configurations.

Figure 10.- Effect of nose blunting on transition Reynolds number.

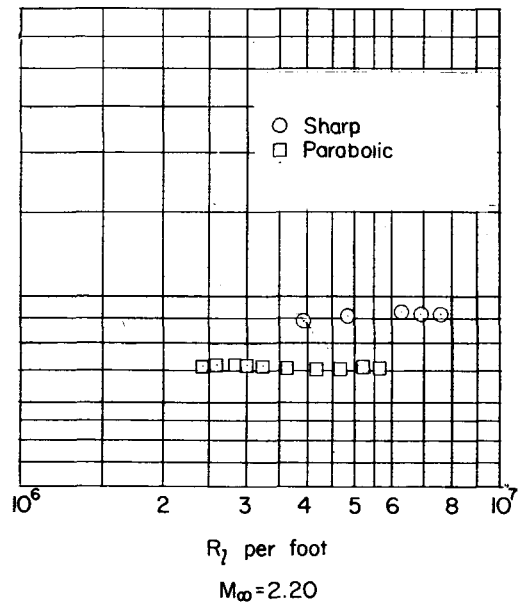
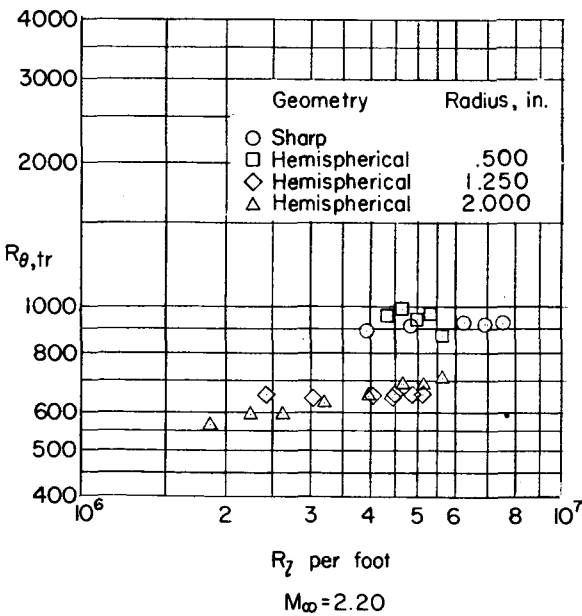


(a)  $27^\circ$  cone configurations. Concluded.

Figure 10.- Continued.



(b)  $45^\circ$  cone configurations.



(c)  $60^\circ$  cone configurations.

Figure 10.- Concluded.

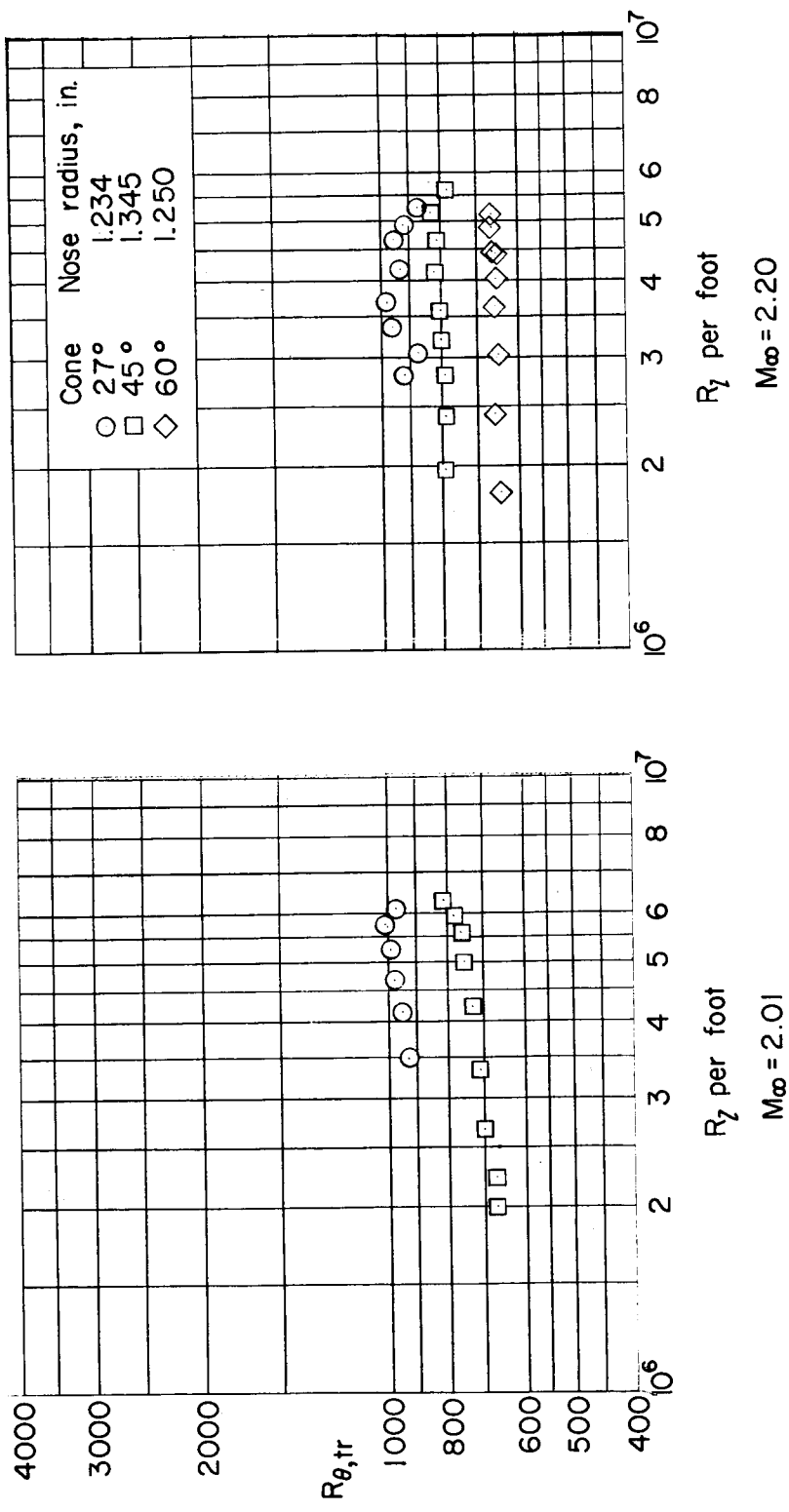


Figure 11.- Effect of cone angle on transition Reynolds number for configurations with approximately the same values of nose radius.

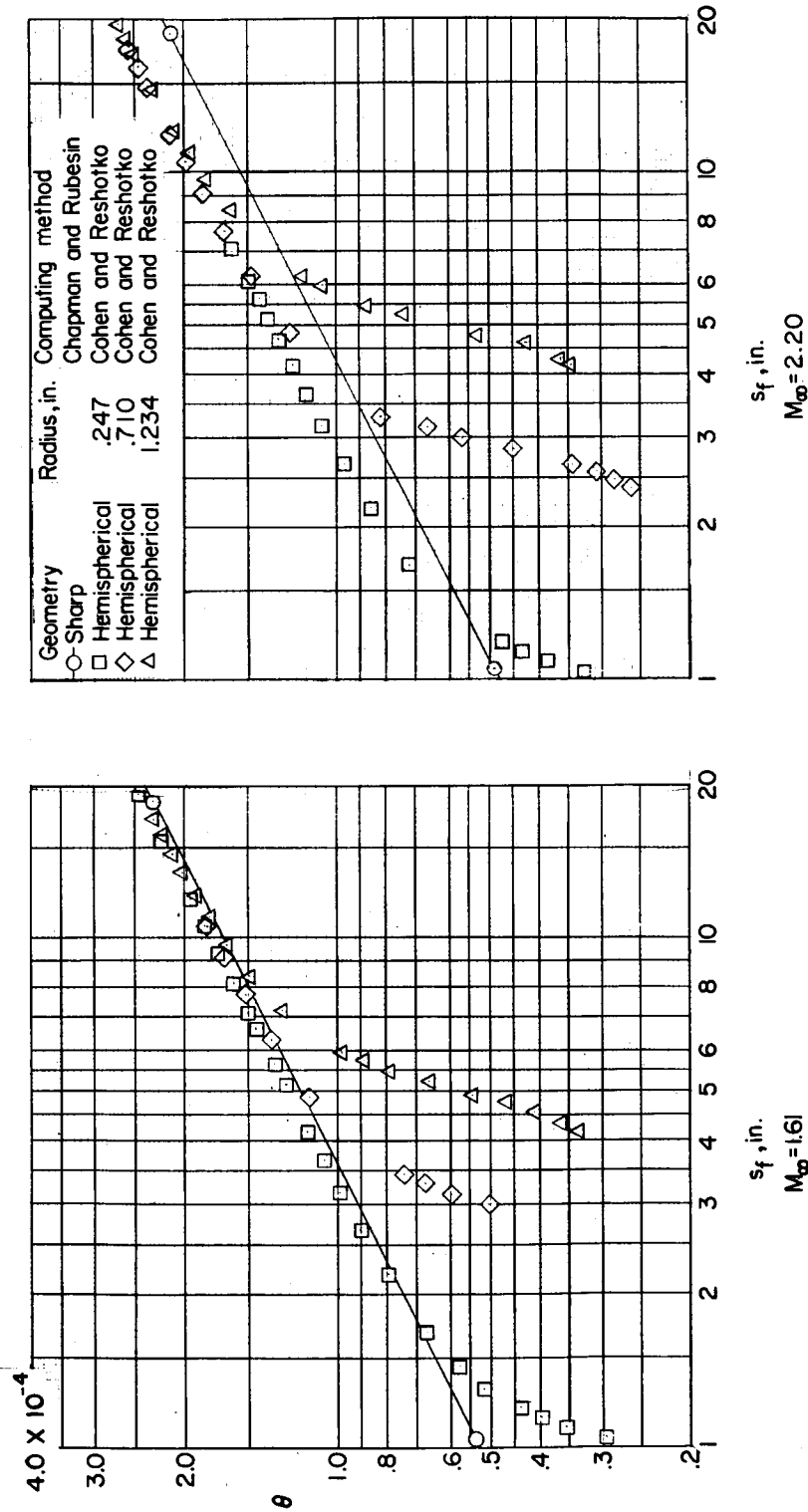


Figure 12.- Momentum-thickness calculations for the 27° cone configurations by the Chapman and Rubesin and the Cohen and Reshotko techniques.